Published in final edited form as:
Biomaterials. 2011 September ; 32(26): 6316–6323. doi:10.1016/j.biomaterials.2011.05.020.

Carbon Nanotube Nanoreservior for Controlled Release of Anti-inflammatory Dexamethasone

Xiliang Luo[a], **Christopher Matranga**[b], **Susheng Tan**[c], **Nicolas Alba**[a], and **Xinyan Tracy Cui**[a,d,e,*]

[a] Department of Bioengineering, University of Pittsburgh, Pittsburgh, PA 15260, USA

[b] Chemistry and Surface Science Division, National Energy Technology Laboratory, U.S. Department of Energy, P.O. Box 10940, Pittsburgh, PA 15236, USA

[c] NanoScale Fabrication and Characterization Facility, Petersen Institute of NanoScience and Engineering, and Department of Electrical and Computer Engineering, University of Pittsburgh, Pittsburgh, PA 15261, USA

[d] Center for Neural Basis of Cognition, University of Pittsburgh, Pittsburgh, PA 15260, USA

[e] McGowan Institute for Regenerative Medicine, University of Pittsburgh, Pittsburgh, PA 15260, USA

Abstract

On demand release of anti-inflammatory drug or neurotropic factors have great promise for maintaining a stable chronic neural interface. Here we report the development of an electrically controlled drug release system based on conducting polymer and carbon nanotubes. Drug delivery research using carbon nanotubes (CNTs) has taken advantage of the ability of CNTs to load large amounts of drug molecules on their outer surface. However, the utility of the inner cavity of CNTs, which can increase the drug loading capacity, has not yet been explored. In this paper, the use of multi-wall CNTs as nanoreserviors for drug loading and controlled release is demonstrated. The CNTs are pretreated with acid sonication to open their ends and make their outer and inner surfaces more hydrophilic. When dispersed and sonicated in a solution containing the anti-inflammatory drug dexamethasone, experiments show that the pretreated CNTs are filled with the drug solution. To prevent the unwanted release of the drug, the open ends of the drug-filled CNTs are then sealed with polypyrrole (PPy) films formed through electropolymerization. The prepared electrode coating significantly reduced the electrode impedance, which is desired for neural recording and stimulation. More importantly, the coating can effectively store drug molecules and release the bioactive drug in a controlled manner using electrical stimulation. The dexamethasone released from the PPy/CNT film was able to reduce lipopolysaccharide induced microglia activation to the same degree as the added dexamethasone.

1. Introduction

Neural prostheses based on implantable microelectrodes have been widely studied to modify, restore, or bypass a damaged or diseased portion of the nervous system. However,

*Corresponding author, xic11@pitt.edu.

the chronic application of these neural electrodes has been limited due to degradation of performance over time, possibly due to the neuronal loss and scar formation through inflammatory tissue reaction [1, 2]. In order to minimize or eliminate the undesirable tissue reaction, strategies such as delivering/releasing anti-inflammatory drugs or neurotrophic factors to the vicinity of the implant are being explored. Drug release systems based on conducting polymers have been extensively studied, as conducting polymers offer the possibility of drug administration through electrical stimulation [3–7]. Electrically controlled release has found many applications [8], and it is particularly attractive for implantable devices such as neural electrode arrays. For example, neural microelectrodes modified with polypyrrole (PPy) or poly(3, 4-ethylene dioxythiophene) (PEDOT) incorporating nerve growth factor (NGF) can effectively deliver NGF to initiate the differentiation of rat pheochromocytoma cells [9]. The anti-inflammatory drug dexamethasone (Dex) has also been shown to be electrically released from PPy and PEDOT to mitigate the inflammatory tissue response [4, 5]. More recently, it was reported that cochlear implant electrodes coated with PPy films incorporating neurotrophin-3 could be used to preserve spiral ganglion neurons through electrically triggered neurotrophin delivery [6]. However, the application of such systems has been limited due to some intrinsic technical barriers. For instance, the drug loading capacity of a conventional conducting polymer film is limited, and the amount of drug release per stimulation is neither steady nor sustainable.

In recent years, carbon nanotubes (CNTs) have attracted considerable attention for their applications in biomedical science and technology [10–13]. It was reported that the functionalized CNTs displayed low toxicity and no immunogenicity [14, 15], because the functionalized CNTs are dispersible in water and compatible with biological fluids, and they can be excreted through the renal route [16]. As CNTs can be functionalized with different molecules, such as proteins, nucleic acids and drugs, various types of drug delivery or controlled release systems based on CNTs have been developed [17, 18]. However, in most of these systems, the substances to be delivered were attached to the CNT surface through covalent or noncovalent binding [19, 20], leaving the inner cavity unutilized. When the ends of CNTs are opened [21, 22], the inner volume of the tubes becomes accessible and can be filled with different drugs, ranging from small molecules to peptides and even proteins. Although early work has reported on the filling of CNTs with water [23], C-60 [24], polystyrene nanobeads [25] and nanoparticles [26, 27], investigations into using the inner CNT cavity to load bioactive drugs are still in an early stage. Among the different methods proposed for loading drug into CNTs [28], the most convenient way is to fill the CNTs using solutions, but the filling efficiency is greatly reduced by the surface tension of the liquid inside the CNT [29]. Likewise, another challenge in using CNTs for drug delivery involves preventing the loaded drug from leaking out of the opened ends of CNTs until a controlled release is required.

Recently, Ajima and coworkers [30–32] have reported on the incorporation of cisplatin inside single-wall carbon nanohorns. Another interesting work was reported by Ren and Pastorin [33], where the antitumor drug hexamethylmelamine was incorporated inside single- and double-wall CNTs. Drug release from the open ends of the tubes was prevented by sealing the CNT with adsorbed C-60, which can later be removed in CH_2Cl_2 for a more controlled release. While these studies illustrate some of the recent progress in this area, there are still many fundamental and practical issues regarding the controlled loading and release of drugs from CNTs which must be addressed to make this a viable and useful technology. In particular, improving the amount of drug released, increasing the stability/lifetime of the releasing films, utilizing the unique porosity of the CNTs for storage/release, and providing mechanistic insight into the drug release process are still key issues that need to be addressed in these systems.

Herein, we report the use of multi-wall CNTs as nanoreserviors for drug delivery. CNTs were sonicated in strong acids to break them into shorter tubes and open their ends. The pretreated hydrophilic CNTs were then filled with a Dex solution. To make CNT nanoreserviors, the drug loaded CNTs were encapsulated in PPy films through electropolymerization. The drug loaded in the PPy/CNT composite film can be efficiently released upon electrical stimulation. The CNTs served as nanoreserviors of Dex, provided a higher drug loading capacity, and possessed a more linear and sustainable release profile than that of a conventional PPy film.

2. Materials and Methods

2.1. Materials

Pyrrole (98%) was purchased from Sigma-Aldrich, vacuum distilled and stored frozen. Dexamethasone (Dex) 21-phosphate disodium salt was purchased from Sigma-Aldrich. Two types of multi-wall CNTs were used in this work, CNTs a (CNTa, outer diameter 110–170 nm, inner diameter 3–8 nm, length 5–9 μm, purity > 90%) were purchased from Sigma-Aldrich, and CNTs b (CNTb, outer diameter 20–30 nm, inner diameter 5–10 nm, length 10–30 μm, purity > 95%) were purchased from Cheap Tubes Inc. (Brattleboro, USA). Phosphate buffered saline (PBS, pH 7.4) was purchased from Sigma-Aldrich, and the used PBS contain 10 mM sodium phosphate and 0.9% NaCl. All other chemicals were of analytical grade, and Milli-Q water from a Millipore Q water purification system was used throughout.

2.2. Apparatus

Electrochemical experiments were performed on a Gamry Potentiostat, FAS2/Femtostat (Gamry Instruments) with Gamry Framework software. A conventional three-electrode system with the glassy carbon (GC) electrode as the working electrode, a platinum wire as the counter electrode, and a silver/silver chloride (Ag/AgCl) reference electrode (CH Instruments) was used. Scanning electron microscopy (SEM) was performed with an XL30 SEM instrument (FEI Company), with an accelerating potential of 10 kV and a working distance of 10 mm. The samples for SEM were prepared on self-prepared GC electrode (made of GC rod with the diameter of 3.0 mm). Transmission electron microscopy (TEM) was performed with a JEOL JEM2100F TEM instrument (JEOL Inc., Japan). The concentration of Dex solution was measured with a microplate reader SpectraMax M5 (Molecular Devices), using the ultraviolet (UV) absorption of Dex at 242 nm. A Beckman L8-80M ultracentrifuge was used for the centrifugation of CNT suspensions.

2.3. Electron energy loss spectra

The electron energy loss spectra (EELS) were obtained using a JEOL JEM2100F TEM (JEOL Inc., Japan) operating at an accelerating voltage of 200 kV and equipped with a Tridiem GIF post-column imaging filter (Gatan Inc) [34]. EELS data were recorded at 200 kV using an energy dispersion of 0.5 eV. The spectra were acquired using ‘image-diffraction’ mode at a beam size of about 5 nm at either the edge or core areas of CNTs and processed by means of Digital Micrograph software (Gatan Inc., Warrendale, PA).

2.4. Specific Surface Area measurements

The specific surface area of CNTs was measured with a Quantachrome Autosorb instrument using a 5 point N_2 BET measurement for a P/P_o range of 0.1–0.3. Four runs were conducted for each sample to determine the standard deviations reported in the text. Additional runs on other batches of CNTs give nearly identical surface area values.

2.5. X-ray photoelectron spectroscopy

The X-ray photoelectron spectroscopy (XPS) was done with a PHI5600ci instrument using Al Kα X-rays (1486.6 eV) and a pass energy of 187.85 for survey scans and 58.70 eV for higher resolution scans of the C 1s, O 1s, and Mo 3d regions. Sample powder was placed into a machined well in a Mo sample holder. The integrated intensities from high resolution scans of the the C and O regions were normalized to the Mo 3d integrated intensity obtained from the Mo sample holder. A small spot sputter source was used to clean the analysis area of the molybdenum holder of any oxide or adventitious carbon. As the CNTs are conductive, no sample charging was noted during the analysis. The C and O integrated were also normalized to account for the different atomic sensitivity factors (ASFs) associated with these two elements.

2.6. Electrochemical impedance spectroscopy

The electrochemical impedance spectroscopy (EIS) was measured with the Gamry Potentiostat, FAS2/Femtostat (Gamry Instruments) with Gamry Framework software using a three-electrode system. The solution for the EIS measurement was 0.1 M KCl containing 10 mM $[Fe(CN)_6]^{3+/4+}$. The EIS was measured in the frequency range from 0.5 Hz to 100K Hz using an applied AC voltage of 5 mV, and recorded at 10 points/decade.

2.7. Loading drug into CNTs

The CNTs were firstly pretreated by dispersing 200 mg CNTs in 100 mL 1:3 concentrated HNO_3 and H_2SO_4 solution and sonicating for 2 hours. The suspension was then kept at room temperature overnight. After the acid treatment, the CNTs were washed with water and separated using ultracentrifuge repeatedly until the pH of the washing solution was neutral. Finally, the CNTs were collected and dried at 60 °C. To the solution of 20 mg/mL Dex in water, 1.0 mg/mL pretreated CNTs were added, and the resulted mixture was sonicated for 2 hours to let the Dex solution enter the inner cavity of CNTs.

2.8. Preparation of drug-loaded PPy films

GC electrodes (3 mm in diameter) were polished with 1.0, 0.3 and 0.05 μm alumina slurries in sequence and then ultrasonically washed in water and ethanol for about 5 min, respectively. 0.4 M pyrrole was added to the above Dex solution containing drug-loaded CNTs (20 mg/mL Dex and 1 mg/mL CNTs), and the cleaned GC electrodes were immersed into the suspension for electropolymerization. The electropolymerization of pyrrole was carried out at a constant current of +70 μA for 400 s, and PPy films incorporated with Dex and drug-loaded CNTs were thus formed. For comparison, conventional PPy films without CNTs but incorporated with Dex were electropolymerized with similar ways in the solution containing only 0.4 M pyrrole and 20 mg/mL Dex.

2.9. Electrochemically controlled drug release

After electrodeposition, the PPy films with and without CNTs were thoroughly washed with water, and then soaked in 10 mM PBS for 15 min under magnetic stirring to entirely remove the adsorbed Dex. The electrochemically controlled release of drug from the PPy films was carried out in a small electrochemical cell containing 1.6 mL 10 mM PBS (pH 7.4). A square wave electrical stimulation with 50% duty cycle was used for drug release. The applied potentials were −2.0 V for 5 s followed by 0.0 V for 5 s (aggressive stimulation, for quick drug release), or −0.5 V for 5 s followed by 0.5 V for 5 s (mild stimulation, for sustainable drug release). The solution with the released drug was sampled after 10 cycles (stimulation times) or more cycles of square wave electrical stimulation specified in each experiment description. The solution with released drug was then transferred to 96 well

Costar assay plate and used for UV absorption measurement at 242 nm. Drug diffusion was tested with similar procedure, but without actually applying the electrical potential.

2.10. Assessment of the bioactivity of the release drug

In order to assess the bioactivity of the released Dex, both released Dex and bulk-purchased Dex solutions were used to supplement cultures of Highly Aggressively Proliferating Immortalized (HAPI) cells [35] together with gram-negative bacteria-derived lipopolysaccharide (LPS, from Escherichia coli 0111:B4, Sigma). Nitrite content within a supernatant prepared from each culture was then determined using a Griess reagent kit (G-7921, Invitrogen, Carlsbad, CA), to determine the relative nitric oxide production rates between the two varieties of Dex and control cultures prepared using sterile PBS in place of either Dex or Dex as well as LPS.

The experiment was performed by dividing the cultured cells into six groups of three wells each: a control group, an LPS treated group, an LPS plus released Dex treated group, an LPS plus control Dex treated group, and a sham release control and an LPS plus sham release control group. Sham release control contains the PBS that was exposed to Dex-free films subjected to release stimulation, to verify that films do not release additional confounding impurities during stimulation. A concentrated solution of released Dex was prepared by electrically stimulating 6 PPy/CNTb/Dex film coated electrodes in sterile PBS (each for one hour in the same solution using aggressive stimulation). For the sham control experiments, 6 Ppy/CNTb film (no Dex) coated electrodes were stimulated similarly in sterile PBS. A control Dex solution was prepared by adding bulk purchased Dex powder to sterile PBS to an equivalent concentration as that within the released Dex solution. A concentrated LPS solution was prepared by reconstituting LPS powder in sterile PBS. Media compositions were prepared for each of the six experimental groups: Each group was prepared by adding concentrated LPS, fetal bovine serum (FBS, Invitrogen, Carlsbad, CA), and either released or control Dex solutions to DMEM (Gibco 21041 DMEM/F12 +L-glutamine − HEPES − Phenol Red, Invitrogen, Carlsbad CA) to make final concentrations of 1 μg/ml LPS, 10% FBS, and 10 μM of either released or control dexamethasone. The LPS group consisted of the same composition as above, only with an equivalent volume of sterile PBS in place of the concentrated Dex solution. The control group consisted of the same composition, only with an equivalent volume of sterile PBS in place of both the concentrated LPS and Dex solutions. The sham release control and LPS media compositions were prepared as above, only replacing the pure sterile PBS with the sham release PBS prepared in the initial steps.

Frozen HAPI cells (provided courtesy of Dr. Xiaoming Hu, Department of Neurology, University of Pittsburgh) were thawed and passaged once before being plated at a density of 1×10^4 cells/well in a 24-well plate. Cells were plated within the treatment solutions prepared above, with 3 wells allocated to each treatment, randomly distributed around the well plate to avoid positional bias. Plated cell cultures were incubated in treatment media for 24 hours at 37°C, after which the media of each well was sampled for analysis. NO production of each culture was approximated by measuring sample nitrite content using a Griess reagent kit and reading absorbance at 540 nm using a Molecular Devices Spectramax M5 plate reader. The concentration of nitrite in each sample was determined by comparing measured values against a standard curve generated using a series of known concentrations of between 1–100 μM nitrite. Additional measurements were collected from control samples of fresh media and PBS containing the Griess reagent solutions. After media was sampled for analysis, wells were stained using MTT assay (Vybrant® MTT Cell Proliferation Assay Kit V-13154, Invitrogen, Carlsbad, CA) to quantify cell count. The reported amounts of nitrite production for each condition were normalized by the cell count. Significance of difference of nitrite production between the various treatment groups was determined using a one-way ANOVA with Tukey's post hoc analysis, employing a significance level of 0.05.

3. Results and Discussion

3.1. Acid Sonication of the CNTs

In order to provide access to the CNT inner cavity, as shown in Scheme 1, the CNTs must have at least one end open. As synthesized CNTs will typically have closed ends, but depending on the harvesting process, the tubes may possess some open ends [36]. In order to more fully open the ends of the CNTs, two samples (CNTa, outer diameter 110–170 nm, inner diameter 3–8 nm; CNTb, outer diameter 20–30 nm, inner diameter 5–10 nm) were treated with acid (1:3 concentrated HNO_3 and H_2SO_4) under sonication for 2 h.

It has been reported that the acid treatment together with sonication will cause severe etching of the graphitic surfaces (both outer and inner) of the CNTs, resulting in tubes of shorter length with opened ends [37, 38]. Transmission electron microscopy (TEM) of the acid treated samples verified the shortened tube length after treatment and the presence of open ends (Figure S1). The opening of CNT ends is also verified by increases in the specific surface area (SSA) determined with a 5 point N_2 BET measurement before and after treatment. After the acid sonication, the SSA of CNTa increased from 12.93 (± 0.29) to 24.14 (± 0.19) m^2/g and the SSA of CNTb changed from 111.73 (± 0.52) to 126.64 (± 0.90) m^2/g. The SSA of CNTa increased by about 86.7%, which is similar to previous reports [39]. The SSA of CNTb only increased by 13.3%, which may indicate that the raw CNTb already possessed some open ends or that this sample was not as reactive to the acid sonication. To confirm that the SSA changes are from true porosity changes (e.g. opening of CNT ends) and not from the simple dissolution of residual metal catalyst in the sample, thermogravimetric analysis (TGA) was performed in air up to 1000 °C. TGA finds ~2.0–2.8 weight % of residual mass in both the treated and untreated samples after ashing in air. This residual mass is presumably from trace amounts of metal co-catalyst in the sample which is converted to metal-oxide during the ashing step. These values are in agreement with the technical data sheets provided by the vendor for these CNTs. We note that this residual mass could also result from other, non-combustible, trace impurities in the sample, although XPS analysis (see below) detects no such species.

Acid treatment is also known to chemically oxidize CNT carbon, produce oxygen containing functional groups (mainly carboxyl), and remove heavy metal catalyst particles. The O and C ratios of the sample are characterized by X-ray photoelectron spectroscopy (XPS) survey scans before and after treatment (Figure 1). The XPS survey scans show the presence of both carbon and oxygen and no evidence of other impurities or residual metal catalyst. The kinetic energy (KE) of detected photoelectrons (KE~1000 eV) for the C 1s peak using our X-ray source indicates that we are probing ~ 21–27 Å into the sample or ~ 6–8 graphitic layers. As such, any residual catalyst encapsulated in a thick carbon shell would not be detected by XPS. This explains why the TGA results find evidence for residual catalyst in the sample ash, but XPS does not detect this metal. From Figure 1, one can qualitatively see higher O/C peak ratios in the acid treated samples and the appearance of the KLL oxygen Auger line, which suggests an increased O content. The O/C ratios were quantified using high resolution scans of the C 1s and O 1s regions (not shown), integrating the band intensity, correcting these intensities for atomic sensitivity factors, and normalizing these peaks to the integrated Mo 3d intensity from the sample holder. The atomic O/C ratio for the untreated CNTb sample was ~0.017 while acid treatment increased this value by a factor of 5–6 to ~ 0.10. As the carboxyl groups are highly hydrophilic, the acid treatment will make the CNTs more hydrophilic on both the exterior [40] and interior [41] surfaces, allowing aqueous solution to more easily enter and fill the inner cavity of the CNTs.

3.2. Loading the inner cavity of the CNTs with Dex

As the treated CNTs have open ends and their exterior and interior surfaces are both hydrophilic, it is expected that aqueous solutions containing drug can flow into the inner cavity of CNTs, especially with the help of sonication. To confirm that the drug Dex (in the form of a soluble salt, Dex 21-phosphate disodium) was really loaded into the inner cavity of CNTs, two separate experiments were carried out with the CNTb sample. In the first experiment, 2.0 mg of treated CNTb was dispersed in 2.0 mL of a 20 mg/mL Dex solution and sonicated for 2 hours to load the CNTs with the drug. The resulting Dex-loaded CNT suspension was filtered through a 0.2 μm filter under vacuum and washed with water repeatedly to remove any Dex which may be loosely adsorbed on the outer surface of the CNTs. An ultraviolet-visible (UV, 242nm) absorption spectrum of the rinse solution confirms that the loosely bound Dex has been rinsed from the CNTs. The Dex containing CNTs were then transferred to a glass bottle filled with 1.2 mL phosphate buffered saline (PBS, pH 7.4, 10 mM phosphate and 0.9% NaCl) and sonicated for 20 min to partially release the loaded drug, and the obtained CNTs suspension was collected and centrifuged (10 min at 13,000 rpm) repeatedly to separate the solid nanotubes from solution. The clear supernatant solution was then collected and measured with UV absorption, and significant UV absorption of Dex was detected, which indicated the presence of Dex in the solution (6.55 ± 0.27 μg). A similar test was carried out with the Raw CNTb, and less Dex was detected (3.89 ± 0.19 μg) in the released solution.

It is expected that some Dex molecules may adsorb on the hydrophobic surface of the Raw CNTs, as the phenanthrene group of Dex will strongly interact with the pi-pi network of the CNTs. After acid treatment, the CNTs will become more hydrophilic and possess a negative charge in the PBS (pH 7.4), which can partially prevent the adsorption of negatively charged Dex molecules. Therefore, the adsorption of Dex molecules on the treated CNTb should be less than that on the raw CNTb. While contrarily, the measured drug released from the treated CNTb was 68.3% more than that from the latter, which indicates that the additional Dex here most likely originates from the inner cavity of the CNTs, though some of the Dex inside the CNTs may have been lost during the filtration and washing process. The interpretation of endohedrally bound and released Dex is supported by the BET surface area measurements which show that the treated CNTs have a higher SSA than untreated samples, presumably as a result of access to the inner pore of the tube.

Further verification of Dex loading in the CNTs was carried out using electron energy loss spectroscopy (EELS) which is integrated with the TEM instrument. EELS is sensitive to light elements, capable of analyzing a small quantity of material, and can spatially probe samples down to a spot size of 1 nm diameter or smaller [42]. A drop of suspension containing Dex loaded CNTb was put on the Cu grid and allowed to dry. The grid was then rinsed in water three times to remove the loosely adsorbed Dex from the outer surface of the tube and from the grid itself. EELS were recorded from the edge and core areas of CNTb with a beam size of about 5 nm, respectively. As shown in Figure 2, we see clear $L_{2,3}$ core loss of carbon for both the edge and core areas of the CNTs, while the $L_{2,3}$ core loss of phosphorous was only observed on the EELS acquired at the core area of the drug loaded CNTs, but not on those spectra at the edge of those CNTs. EELS results were reproducible on several different samples. As the Dex used here is, dexamethasone sodium phosphate, the presence of a clear P peak in the EELS serves as an additional confirmation of the drug's presence inside the tubes.

3.3. Sealing the open ends of the CNTs with electropolymerization of PPy

To keep the loaded Dex inside the CNTs, an electropolymerized PPy film was used to seal the tubes. When electropolymerization was carried out after adding pyrrole monomer to the

suspension containing Dex and CNTs, some of the CNTs may be incorporated in the deposited PPy film as co-dopants with Dex or via physical entrapment [43]. Figure 3 shows the scanning electron microscope (SEM) images of polymerized PPy films containing CNTa and CNTb on glassy carbon (GC) electrodes. As can be seen, in both cases the CNTs were well distributed within the PPy films, and the PPy/CNTb film is more uniform than the PPy/CNTa film. In addition, it can be seen that the PPy films prefer to grow around the CNTs due to the high conductivity of CNTs, and the opened ends of CNTs are well sealed. This result is similar to a previous report [43].

Since the CNTs were filled with Dex solution in their inner cavities, once the PPy film is formed around the CNTs, the Dex will become sealed inside the CNTs. The effective sealing of the open ends of CNTs was verified by a diffusion test in phosphate buffered saline (PBS, pH 7.4, 10 mM phosphate and 0.9% NaCl), as compared to the controlled release initiated with electrical stimulation, the amount of Dex which diffused from the PPy/CNTs film to the PBS was negligible (see Figure S2 in supporting information).

The electrical properties of drug-loaded CNTs on the PPy films were studied using electrochemical impedance spectroscopy (EIS), which measures frequency-dependent changes in impedance. As shown in Figure 4, coating the GC electrode with PPy led to a decreased impedance, due to the increased effective surface area of the electrode from the polymer film [44]. Interestingly, the addition of CNTs to the PPy film led to a decreased impedance at all frequencies (0.5 to 100K Hz), and the impedance of PPy film with CNTb was even lower than that of the PPy film with CNTa. This decrease in impedance may be ascribed to two reasons. One is related to the increased surface area of the PPy/CNT film. As shown in Figure 3, the PPy films incorporated with CNTs exhibited a fibrous morphology. The other reason for the decreased impedance is the increased conductivity of the PPy film, as CNTs are highly conductive, and their incorporation in PPy films can effectively increase the conductivity of the latter [43]. Since the CNTb tubes have a smaller diameter than those in CNTa, this sample can form finer nanostructures with higher surface/volume ratios. Moreover, the thinner CNT can be better distributed in the PPy film to make it more conductive. Therefore, compared to CNTa, CNTb is more effective in decreasing the impedance of the PPy film.

3.4. Electrically controlled release of Dex

Electrochemically controlled drug release from PPy films has been previously studied. The mechanism of release is mainly attributed to the de-doping process during negative bias that electrochemically reduces the positively charged polymer backbone to a neutral state causing the release of negatively charged drug from the film. Since the Dex-loaded CNTs were incorporated in the PPy film as drug nanoreserviors, it is expected that the PPy film with incorporated CNTs can load and release more drug than the pure PPy film. The total amount of releasable drugs from different polymer films was measured and compared, as shown in Figure 5. The electrically controlled drug release of different PPy films was tested in 10 mM PBS with an aggressive electrical stimulation (repeated stimulation of −2 V for 5 s followed by 0 V for 5 s) successively for 20 hours, and the amount of released drug was measured. After electrical stimulation for 20 hours, we have further stimulated the film for one hour and observed no more drug release. Therefore we can conclude that all releasable drug has been delivered within the 20 hours of aggressive stimulation. The PPy films with CNT drug nanoreserviors release more drug than the film without CNTs, and the drug released from the PPy/CNTb film was more than that from the PPy/CNTa film (the amount of released Dex from systems based on pure PPy, PPy/CNTa and PPy/CNTb are 38.8 ± 3.2, 53.3 ± 1.7 and 78.7 ± 2.1 μg, respectively).

As the amount of releasable drug from different PPy films is closely related to the amount of drug loaded in the corresponding PPy films, the above results indicate that the PPy films incorporated with CNTs have a higher drug capacity than the pure PPy film. Since the PPy films with and without CNTs were synthesized under similar conditions using the same charge, the amount of deposited PPy should be nearly identical. Therefore the increased drug load is attributed to the incorporation of CNTs carrying extra drug. This higher loading is attributed to the thinner outer diameter and wider inner diameter of the tubes in CNTb giving this sample a higher drug capacity per unit weight than CNTa. As a result of this higher capacity, the PPy/CNTb film can release more Dex than the PPy/CNTa film.

The drug release profile of different systems was studied using a milder stimulus (± 0.5 V) for up to 300 stimulations, and the profiles are shown in Figure 6. As we can see, the drug releasing profile of the PPy/CNTb film is nearly linear within the 300 stimuli, while that of the pure PPy film is curved and levels off. As we know, during electrical stimulation the drug molecules dissociated from the backbone will be released from the bulk PPy film to its surroundings under electrical (charge repulsion) and diffusional force. For the pure PPy film, as the total number of stimulations increases, the concentration of drug in the PPy film decreases, and thus the drug release per stimulus from the pure PPy film decreases and eventually levels off. While for the PPy/CNTb film, the actuation effect of PPy film upon electrical stimulation [45, 46] may cause the expansion or contraction of the polymer, and thus temporarily open the seal on each end of the nanotubes and accelerate the drug release. Therefore, release from the PPy/CNTb film can be more sustainable due to the extra drug stored inside the CNT capsules. A linear release profile is desired for an actively controlled drug delivery system. Based on the release profile of PPy/CNTb, the sample has not exhausted its delivery capacity, which indicates a more sustainable drug release system. Since the drug loading capacity of CNTa is less than that of CNTb, the drug releasing profile of the PPy/CNTa film should be somewhere in between the PPy and PPy/CNTb film, and this was exactly what we have found in the experimental result, as shown in Figure 6.

3.5. Bioactivity of the released Dex

In order to assess the bioactivity of the released Dex, a microglia cell line, HAPI cells were used [35]. HAPI cells can be activated with a pro-inflammatory molecule LPS and activated microglia cells secrete various inflammatory products including nitric oxide (NO) and pro-inflammatory cytokines. When Dex is added in the LPS supplemented microglia culture, the activation of cells can be effectively suppressed and the NO production reduced. Here we employed a technique similar to that described by Hinkerohe et al [47]. Briefly, both released Dex and bulk-purchased Dex solutions with a concentration of 10μM were added to HAPI cell cultures together with LPS. The nitrite content, which is proportional to the NO concentration, of each culture was then determined using a Griess reagent kit. As shown in Figure 7 (in terms of mean ± SD), HAPI cells produced elevated quantities of NO when exposed to LPS, in agreement with observations by Cheepsunthorn et al [35]. Both released and added Dex caused the LPS-stimulated rate of NO production to diminish significantly ($p<0.05$), in a manner similar to glial co-cultures as observed by Hinkerohe et al [47]. The effective inhibition of microglia activation by released Dex indicates that the drug molecules retained their bioactivity after the loading and stimulated release. The cell numbers of each group were checked, and there is no significant difference among them, which indicates that the cell effects found are not caused by a reduced cell number and/or cell death. No significant difference was observed between the control and sham release control groups, or between the LPS and sham release LPS groups, suggesting that all observed effects are due to released Dex, and not from any unidentified impurities that may have been released from the films.

4. Conclusions

An enhanced electrically controlled drug release system based on conducting polymer PPy incorporated with CNT drug nanoreserviors was developed. The CNT drug nanoreserviors, composed of CNTs with Dex loaded in their inner cavity and PPy coatings that seal the ends of CNTs, can effectively load drug and release them in bioactive form under electrical stimulations. The incorporation of CNT drug nanoreserviors can not only significantly increase the amount of loaded and releasable drug of the system, but also provide a more linear and sustainable drug release profile. In addition, the presence of CNTs can lower the impedance of the PPy film, which is a desirable property in applications where the same electrode is expected to perform other functionalities such as electrophysiological recording and/or stimulation.

Supplementary Material

Refer to Web version on PubMed Central for supplementary material.

Acknowledgments

The project described was supported by the National Science Foundation Grant 0748001 and 0729869, National Institute of Health R01NS062019, the Department of Defense TATRC grant WB1XWH-07-1-0716 and DARPA MTO N66001-11-1-4014.

References

1. Roitbak T, Sykova E. Diffusion barriers evoked in the rat cortex by reactive astrogliosis. Glia. 1999; 28:40–8. [PubMed: 10498821]
2. Turner JN, Shain W, Szarowski DH, Andersen M, Martins S, Isaacson M, et al. Cerebral astrocyte response to micromachined silicon implants. Exp Neurol. 1999; 156:33–49. [PubMed: 10192775]
3. Pernaut JM, Reynolds JR. Use of conducting electroactive polymers for drug delivery and sensing of bioactive molecules. A redox chemistry approach. J Phys Chem B. 2000; 104:4080–90.
4. Wadhwa R, Lagenaur CF, Cui XT. Electrochemically controlled release of dexamethasone from conducting polymer polypyrrole coated electrode. J Controlled Release. 2006; 110:531–41.
5. Abidian MR, Kim DH, Martin DC. Conducting-polymer nanotubes for controlled drug release. Adv Mater. 2006; 18:405–9. [PubMed: 21552389]
6. Richardson RT, Wise AK, Thompson BC, Flynn BO, Atkinson PJ, Fretwell NJ, et al. Polypyrrole-coated electrodes for the delivery of charge and neurotrophins to cochlear neurons. Biomaterials. 2009; 30:2614–24. [PubMed: 19178943]
7. Moulton SE, Imisides MD, Shepherd RL, Wallace GG. Galvanic coupling conducting polymers to biodegradable Mg initiates autonomously powered drug release. J Mater Chem. 2008; 18:3608–13.
8. Svirskis D, Travas-Sejdic J, Rodgers A, Garg S. Electrochemically controlled drug delivery based on intrinsically conducting polymers. J Controlled Release. 2010; 146:6–15.
9. Kim DH, Richardson-Burns SM, Hendricks JL, Sequera C, Martin DC. Effect of immobilized nerve growth factor on conductive polymers: Electrical properties and cellular response. Adv Funct Mater. 2007; 17:79–86.
10. Martin CR, Kohli P. The emerging field of nanotube biotechnology. Nat Rev Drug Discovery. 2003; 2:29–37.
11. Bianco A, Kostarelos K, Partidos CD, Prato M. Biomedical applications of functionalised carbon nanotubes. Chem Commun. 2005:571–7.
12. Lu FS, Gu LR, Meziani MJ, Wang X, Luo PG, Veca LM, et al. Advances in Bioapplications of Carbon Nanotubes. Adv Mater. 2009; 21:139–52.
13. Thompson BC, Moulton SE, Gilmore KJ, Higgins MJ, Whitten PG, Wallace GG. Carbon nanotube biogels. Carbon. 2009; 47:1282–91.

14. Dumortier H, Lacotte S, Pastorin G, Marega R, Wu W, Bonifazi D, et al. Functionalized carbon nanotubes are non-cytotoxic and preserve the functionality of primary immune cells. Nano Lett. 2006; 6:1522–8. [PubMed: 16834443]
15. Sayes CM, Liang F, Hudson JL, Mendez J, Guo WH, Beach JM, et al. Functionalization density dependence of single-walled carbon nanotubes cytotoxicity in vitro. Toxicol Lett. 2006; 161:135–42. [PubMed: 16229976]
16. Lacerda L, Bianco A, Prato M, Kostarelos K. Carbon nanotubes as nanomedicines: From toxicology to pharmacology. Adv Drug Deliver Rev. 2006; 58:1460–70.
17. Bianco A, Kostarelos K, Prato M. Applications of carbon nanotubes in drug delivery. Curr Opin Chem Biol. 2005; 9:674–9. [PubMed: 16233988]
18. Bhirde AA, Patel V, Gavard J, Zhang GF, Sousa AA, Masedunskas A, et al. Targeted Killing of Cancer Cells in Vivo and in Vitro with EGF-Directed Carbon Nanotube-Based Drug Delivery. Acs Nano. 2009; 3:307–16. [PubMed: 19236065]
19. Tasis D, Tagmatarchis N, Bianco A, Prato M. Chemistry of carbon nanotubes. Chem Rev. 2006; 106:1105–36. [PubMed: 16522018]
20. Liu Z, Sun XM, Nakayama-Ratchford N, Dai HJ. Supramolecular chemistry on water-soluble carbon nanotubes for drug loading and delivery. Acs Nano. 2007; 1:50–6. [PubMed: 19203129]
21. Tsang SC, Chen YK, Harris PJF, Green MLH. A Simple Chemical Method of Opening and Filling Carbon Nanotubes. Nature. 1994; 372:159–62.
22. Geng HZ, Zhang XB, Mao SH, Kleinhammes A, Shimoda H, Wu Y, et al. Opening and closing of single-wall carbon nanotubes. Chem Phys Lett. 2004; 399:109–13.
23. Rossi MP, Ye HH, Gogotsi Y, Babu S, Ndungu P, Bradley JC. Environmental scanning electron microscopy study of water in carbon nanopipes. Nano Lett. 2004; 4:989–93.
24. Smith BW, Monthioux M, Luzzi DE. Encapsulated C-60 in carbon nanotubes. Nature. 1998; 396:323–4.
25. Kim BM, Qian S, Bau HH. Filling carbon nanotubes with particles. Nano Lett. 2005; 5:873–8. [PubMed: 15884886]
26. Korneva G, Ye HH, Gogotsi Y, Halverson D, Friedman G, Bradley JC, et al. Carbon nanotubes loaded with magnetic particles. Nano Lett. 2005; 5:879–84. [PubMed: 15884887]
27. Castillejos E, Debouttiere PJ, Roiban L, Solhy A, Martinez V, Kihn Y, et al. An Efficient Strategy to Drive Nanoparticles into Carbon Nanotubes and the Remarkable Effect of Confinement on Their Catalytic Performance. Angew Chem-Int Ed. 2009; 48:2529–33.
28. Hilder TA, Hill JM. Modeling the Loading and Unloading of Drugs into Nanotubes. Small. 2009; 5:300–8. [PubMed: 19058282]
29. Ebbesen TW. Wetting, filling and decorating carbon nanotubes. J Phys Chem Solids. 1996; 57:951–5.
30. Ajima K, Yudasaka M, Murakami T, Maigne A, Shiba K, Ijima S. Carbon nanohorns as anticancer drug carriers. Mol Pharmaceutics. 2005; 2:475–80.
31. Ajima K, Yudasaka M, Maigne A, Miyawaki J, Iijima S. Effect of functional groups at hole edges on cisplatin release from inside single-wall carbon nanohorns. J Phys Chem B. 2006; 110:5773–8. [PubMed: 16539524]
32. Ajima K, Murakami T, Mizoguchi Y, Tsuchida K, Ichihashi T, Iijima S, et al. Enhancement of In Vivo Anticancer Effects of Cisplatin by Incorporation Inside Single-Wall Carbon Nanohorns. Acs Nano. 2008; 2:2057–64. [PubMed: 19206452]
33. Ren YP, Pastorin G. Incorporation of hexamethylmelamine inside capped carbon nanotubes. Adv Mater. 2008; 20:2031–6.
34. Aronova MA, Kim YC, Zhang G, Leapman RD. Quantification and thickness correction of EFTEM phosphorus maps. Ultramicroscopy. 2007; 107:232–44. [PubMed: 16979822]
35. Cheepsunthorn P, Radov L, Menzies S, Reid J, Connor JR. Characterization of a novel brain-derived microglial cell line isolated from neonatal rat brain. Glia. 2001; 35:53–62. [PubMed: 11424192]
36. Pan ZW, Xie SS, Chang BH, Sun LF, Zhou WY, Wang G. Direct growth of aligned open carbon nanotubes by chemical vapor deposition. Chem Phys Lett. 1999; 299:97–102.

37. Datsyuk V, Kalyva M, Papagelis K, Parthenios J, Tasis D, Siokou A, et al. Chemical oxidation of multiwalled carbon nanotubes. Carbon. 2008; 46:833–40.

38. Rosca ID, Watari F, Uo M, Akaska T. Oxidation of multiwalled carbon nanotubes by nitric acid. Carbon. 2005; 43:3124–31.

39. Delhaes P, Couzi M, Trinquecoste M, Dentzer J, Hamidou H, Vix-Guterl C. A comparison between Raman spectroscopy and surface characterizations of multiwall carbon nanotubes. Carbon. 2006; 44:3005–13.

40. Tessonnier JP, Ersen O, Weinberg G, Pham-Huu C, Su DS, Schlogl R. Selective Deposition of Metal Nanoparticles Inside or Outside Multiwalled Carbon Nanotubes. Acs Nano. 2009; 3:2081–9. [PubMed: 19702319]

41. Kyotani T, Nakazaki S, Xu WH, Tomita A. Chemical modification of the inner walls of carbon nanotubes by HNO3 oxidation. Carbon. 2001; 39:782–5.

42. Egerton RF, Malac M. EELS in the TEM. J of Electron Spectrosc Relat Phenom. 2005; 143:43–50.

43. Chen GZ, Shaffer MSP, Coleby D, Dixon G, Zhou WZ, Fray DJ, et al. Carbon nanotube and polypyrrole composites: Coating and doping. Adv Mater. 2000:522–6.

44. Cui XY, Hetke JF, Wiler JA, Anderson DJ, Martin DC. Electrochemical deposition and characterization of conducting polymer polypyrrole/PSS on multichannel neural probes. Sensor Actuat a-Phys. 2001; 93:8–18.

45. Smela E, Inganas O, Lundstrom I. Controlled Folding of Micrometer-Size Structures. Science. 1995; 268:1735–8. [PubMed: 17834992]

46. Pedrosa VA, Luo XL, Burdick J, Wang J. “Nanofingers” based on binary gold-potypyrrole nanowires. Small. 2008; 4:738–41. [PubMed: 18537136]

47. Hinkerohe D, Smikalla D, Schoebel A, Haghikia A, Zoidl G, Haase CG, et al. Dexamethasone prevents LPS-induced microglial activation and astroglial impairment in an experimental bacterial meningitis co-culture model. Brain Res. 2010; 1329:45–54. [PubMed: 20230803]

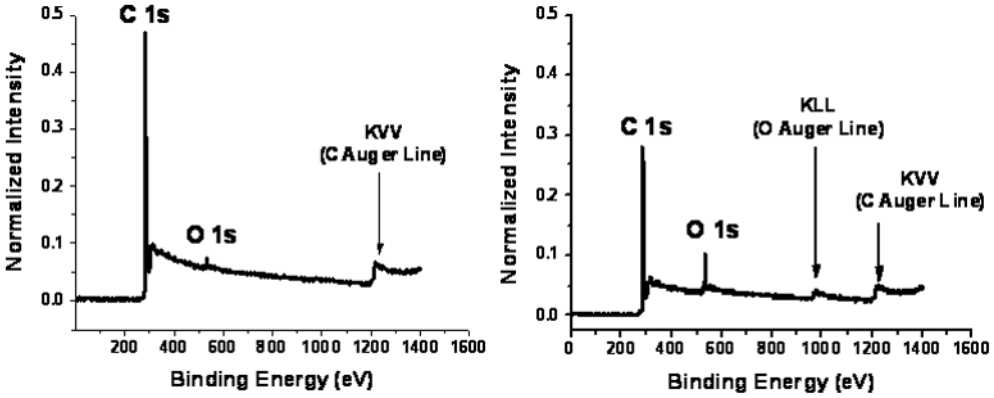

Figure 1.
Normalized X-ray photoelectron spectroscopy spectrum of CNTs before (left) and after (right) acid treatment.

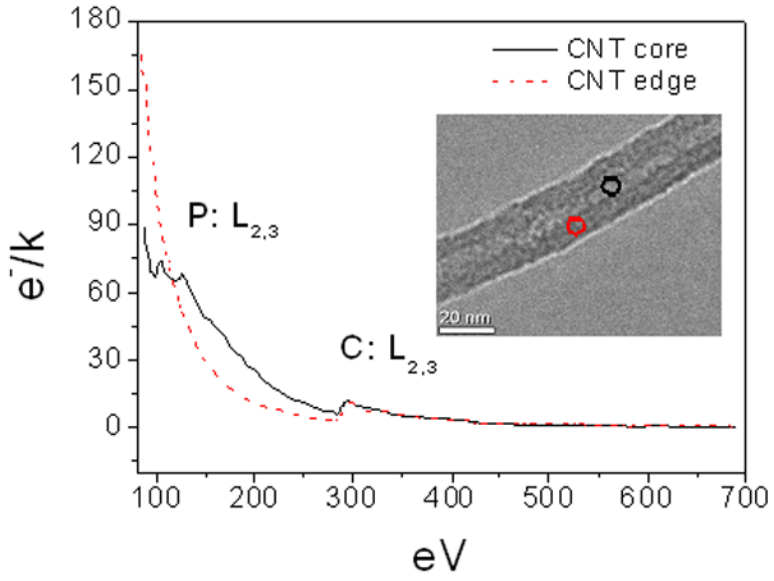

Figure 2.

Electron energy loss spectra of the edge and core areas of drug loaded CNTs. Inset shows a typical TEM image of the CNTb, where the two circles indicate the edge and core area of the nanotube.

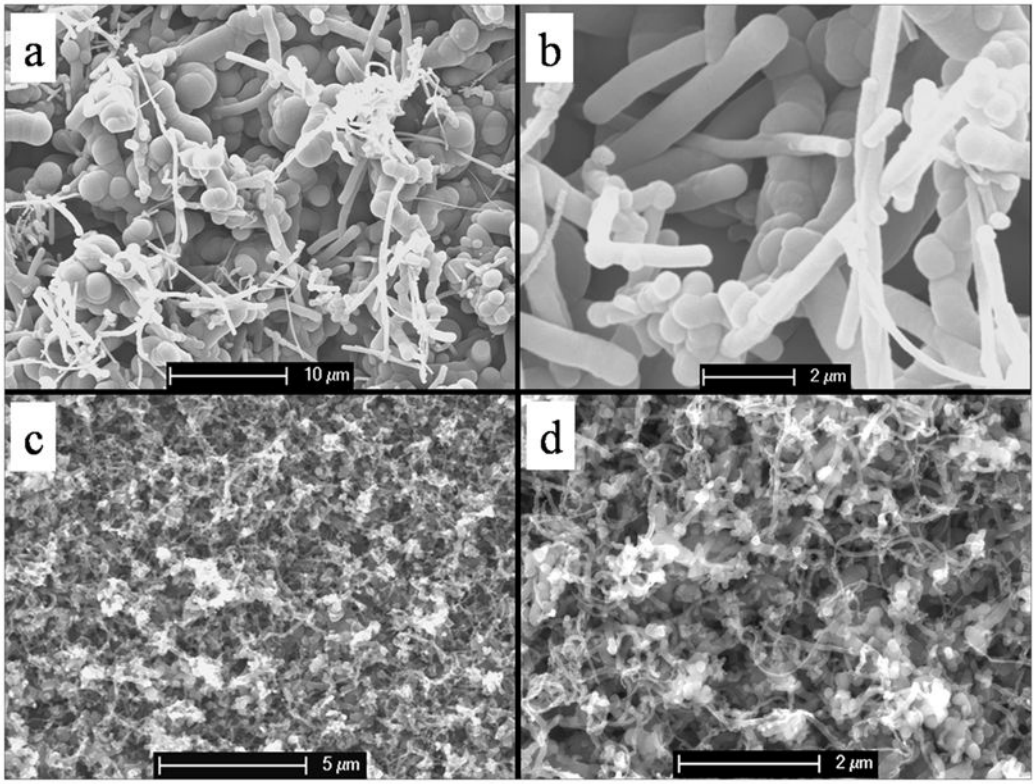

Figure 3.
SEM images of the PPy/CNTa film (a, b) and the PPy/CNTb film (c, d). CNTa: outer diameter 110–170 nm, inner diameter 3–8 nm; CNTb: outer diameter 20–30 nm, inner diameter 5–10 nm.

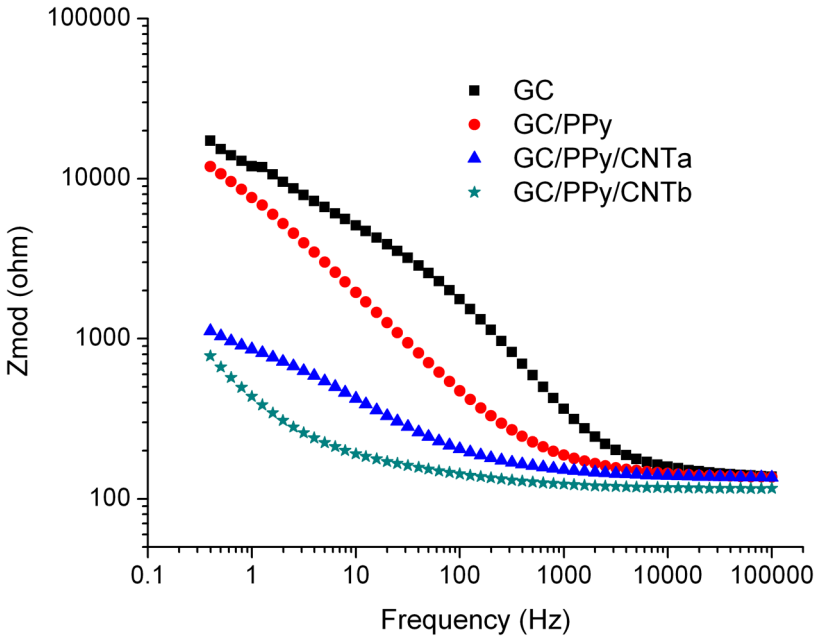

Figure 4.

Electrochemical impedance spectroscopy of different electrodes in the solution containing 10 mM $[Fe(CN)_6]^{3+/4+}$ and 0.1 M KCl. The measurements are performed with a three-electrode system, the frequency range is from 0.5 Hz to 100K Hz, and the applied AC voltage is 5 mV.

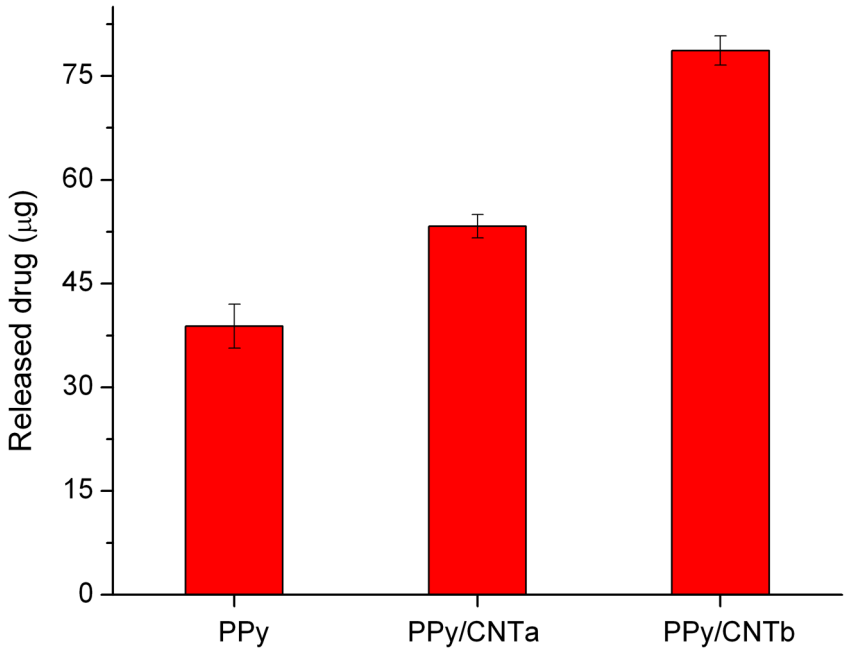

Figure 5.
Dex released from different PPy films under electric stimulation for 20 hours. The electric stimulation applied: 50% duty cycle of square wave, −2 V for 5 s followed by 0 V for 5 s. Data are shown with a ± standard deviation (n = 3 for each case).

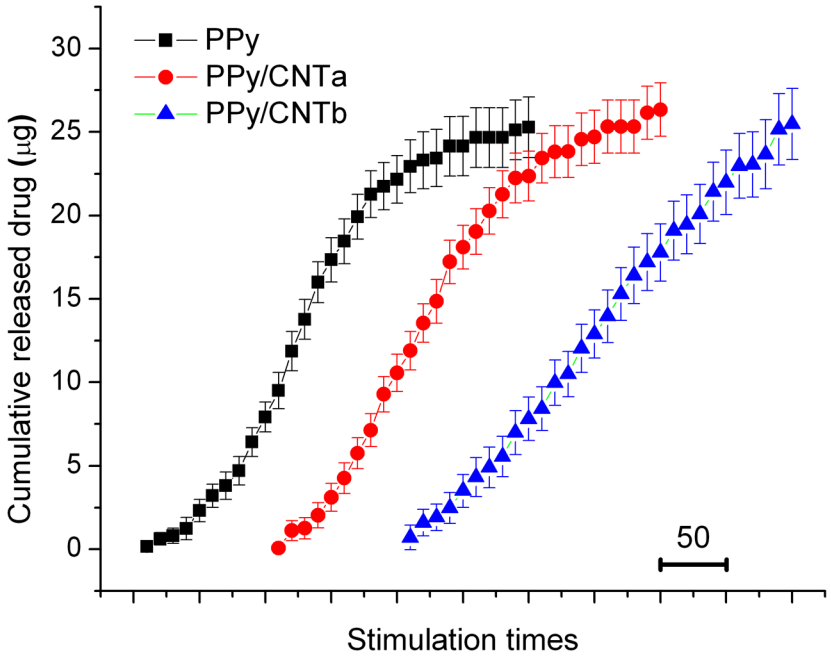

Figure 6.

Dex releasing profiles of different controlled drug release systems for 300 stimulation times. For each stimulation time, the applied stimulus was −0.5 V for 5 s followed by 0.5 V for 5 s, and the solution was sampled every 10 stimulation times. Data are shown with a ± standard deviation (n = 3 for each case).

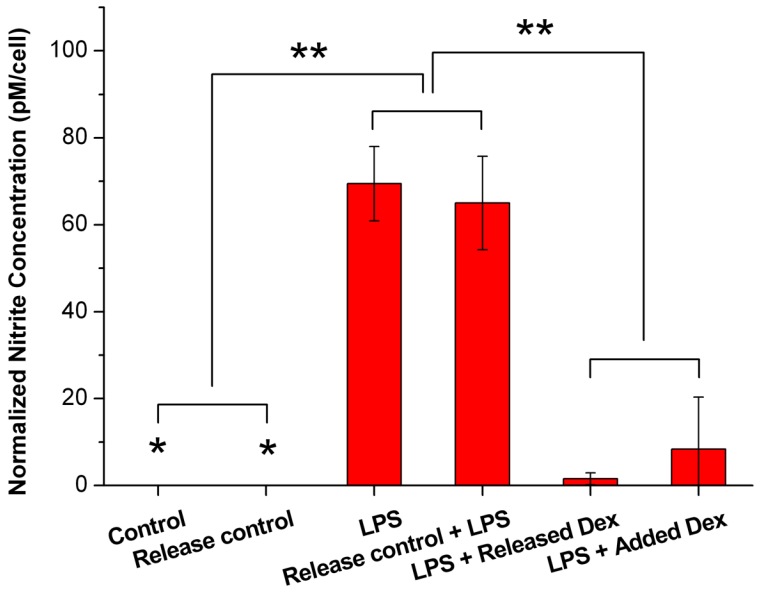

Figure 7.

Comparison of nitrite production of HAPI cell culture preparations following different treatments. Nitrite production provides an indicator of the degree of activation of the cells by LPS. Exposure to media treated with 1μg/ml gram-negative bacteria-derived LPS for 24 hours significantly increased the nitrite production. The added Dex and released Dex groups both showed effective reduction of nitrite production compared to the LPS group, an effect consistent with the bioactivity of the Dex. Data are shown with a ± standard deviation (n = 3 for each case). * indicates there is no detectable nitrite; **, $p < 0.05$.

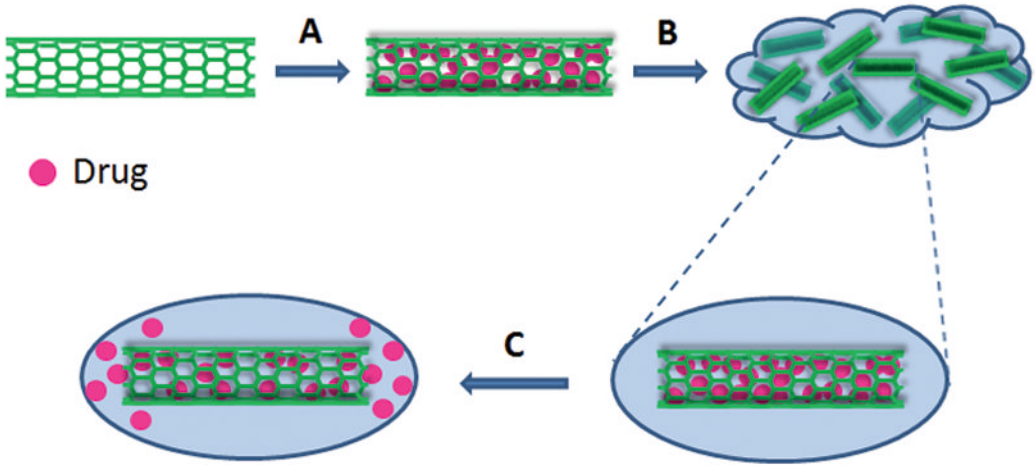

Scheme 1.

Schematic of the drug loading and release process of CNT nanoreservoirs. A) Drug solution is filled into the interior of acid treated CNTs through sonication; B) Pyrrole is added to the suspension containing CNTs and Dex and electropolymerization is carried out; C) Drug is released from CNT nanoreservoirs to surroundings through diffusion or electric stimulation.